J Cardiovasc Pharmacol Therapeut 2(1):27–38, 1997

Experimental Investigations

d-Sotalol Induces Marked Action Potential Prolongation and Early Afterdepolarizations in M but Not Epicardial or Endocardial Cells of the Canine Ventricle

Serge Sicouri, MD, Sandra Moro, Marcelo V. Elizari, MD

Background: Despite its class III antiarrhythmic actions, experimental and clinical studies have shown that *d*-sotalol can also be proarrhythmic; a recent clinical trial that evaluated *d*-sotalol in postmyocardial patients (SWORD) had to be prematurely interrupted because of the excess mortality in the treated group. Previous studies have demonstrated the existence of a marked heterogeneity across the ventricular wall; epicardial, endocardial, and M cells have been shown to display distinct electrophysiologic characteristics and pharmacologic behavior. The present study was designed to test the hypothesis that M cells are the primary target for the class III actions of *d*-sotalol in canine ventricular myocardium and may contribute to its proarrhythmic effects.

Methods and Results: We used standard microelectrode techniques to record transmembrane activity from endocardial, epicardial, midmyocardial, and transmural strips isolated from the canine left ventricle. *d*-Sotalol (100 μM, 60 minutes of exposure, $[K^+]o = 4$ mM) prolongs the action potential in the three cell types, but more so in M than epicardial or endocardial cells, especially at the slower rates. At a basic cycle length of 2000 ms, action potential duration after 90% repolarization increases from 199 ± 20 to 247.5 ± 28 ms in epicardium (n = 10), from 212 ± 26 to 274 ± 27 ms in endocardium (n = 11), and from 309 ± 65 to 533 ± 207 ms in M cells (n = 13). *d*-Sotalol produces a marked steepening of action potential duration-rate relationships of M cells and an upward shift of restitution of action potential duration curves, more accentuated in M cells. Early afterdepolarizations were observed at slow rates (basic cycle lengths > 1000 ms) in 7 of 13 M cell preparations (54%) but not in endocardial or epicardial preparations. A sudden acceleration of the rate could also induce a transient prolongation of the action potential and early afterdepolarization activity.

Conclusion: In canine ventricular tissues, *d*-sotalol manifests its class III effects preferentially in the M cells, leading to the development of early afterdepolarizations and a marked increase in transmural dispersion of repolarization. The data suggest an important role of M cells in the proarrhythmic effects of the drug.

Key words: cardiac electrophysiology, cardiac arrhythmias, sotalol, *d*-sotalol, M cells, epicardium, endocardium, early afterdepolarization, triggered activity.

Racemic sotalol (*dl*-sotalol) is a potent, nonselective, β-adrenoreceptor antagonist devoid of local anesthetic action and partial agonist activity. Its dextrorotary isomer, *d*-sotalol, has only minimal β-blocking effects (1).

From the Laboratorio de Electrofisiologia Celular, Divison Cardiologia, Hospital Ramos Mejia, Buenos Aires, Argentina.

Supported by Fundacion Cardiologia Einthoven.

Reprint requests: Dr. Serge Sicouri, Masonic Medical Research Laboratory, 2150 Bleecker Street, Utica, NY 13501.

While *dl*-sotalol has been shown to have antifibrillatory effects, those of *d*-sotalol remain controversial (2,3). Both *dl*- and *d*-sotalol have been shown to be effective in a variety of supraventricular and ventricular arrhythmias (4–7). The antiarrhythmic actions of sotalol are attributed to its class III actions as well as β-adrenergic blockade in the case of *dl*-sotalol. A number of clinical and experimental data have evidenced the prolonging repolarization effects (class III action) of sotalol. In addition to the increase in QT and QTc intervals (8,9),

sotalol has been found to prolong epicardial and endocardial monophasic action potential (MAP) duration in anesthetized dogs (10) and endocardial MAP in humans (11); *in vitro* studies have demonstrated that sotalol induces a concentration-dependent increase in action potential duration (APD) and effective refractory periods in sheep Purkinje fibers; dog Purkinje fibers and ventricular muscle (endocardium); guinea pig sinoatrial node, atrium, and ventricle; human atrium; and rabbit sinus node, atrium, and ventricle (12,13).

In addition to its antiarrhythmic effects, *in vitro* and *in vivo*, experimental data and clinical studies have shown that sotalol can also be arrhythmogenic. Early afterdepolarizations (EADs) have been described in Purkinje fibers exposed to high concentration of *d*-sotalol (14); atypical polymorphic ventricular tachycardias known as torsade de pointes (15) were observed during sotalol infusion in conscious dogs made hypokalemic and bradycardic with permanent complete atrioventricular (AV) block (16) and in patients treated with oral sotalol (17,18). A recent clinical trial involving postmyocardial patients treated with *d*-sotalol (SWORD) had to be interrupted because of the higher mortality observed in the *d*-sotalol group as compared to the control group (19).

Previous studies have demonstrated the presence of a marked heterogeneity in ventricular myocardium; epicardial, endocardial, and M cells have shown important differences in their electrophysiologic characteristics and pharmacologic behavior (20–22). M cells, located in the deep layers of the free wall and subendocardial structures (23,24), typically display a much longer APD than epicardial or endocardial cells at slow rates of stimulation and have been shown to manifest marked action potential prolongation and EADs following exposure to a variety of class III agents (20,25,26).

The present study was designed to test the hypothesis that M cells are the primary target for the class III actions of *d*-sotalol in canine ventricular myocardium and may account for some of the proarrhythmic effects of the drug. Preliminary data have been presented in abstract form (27).

Methods

Experimental Preparation

Endocardial (papillary muscles, trabeculae), epicardial, midmyocardial, and transmural strips (approximately 2.0 × 1.5 × 0.1 cm) were isolated from the left ventricles of hearts removed from anesthetized (sodium pentobarbital, 30 mg/kg) mongrel male dogs. The preparations were isolated using a dermatome (Davol Simon Dermatome, Cranston, RI) to make cuts either parallel or perpendicular (transmural) to the surface of the structures investigated.

The preparations were placed in a tissue bath and allowed to equilibrate for at least 2 hours while superfused with an oxygenated (95% O_2, 5% CO_2) Tyrode's solution (37 ± 0.5°C; pH = 7.35). The composition of the Tyrode's solution was (in mM): NaCl, 129; KCl, 4; NaH_2PO_4, 0.9; $NaHCO_3$, 20; $CaCl_2$, 1.8; $MgSO_4$, 0.5; and D-Glucose, 5.5.

Action Potential Recordings

The tissues were stimulated at basic cycle lengths (BCL) ranging from 500 to 8000 ms using field stimulation or point stimulation (rectangular stimuli 1–3 ms duration, 2.5 times diastolic threshold intensity) delivered through silver bipolar electrodes insulated except at the tips.

Transmembrane potentials were recorded from one or more sites using glass microelectrodes filled with 2.7 M KCl (10–20 Ω DC resistance) connected to a high input-impedance amplification system (World Precision Instruments, Sarasota, FL).

Amplified signals were displayed on Tektronix oscilloscopes and amplified (model 1903-4 programmable amplifiers, Cambridge Electronic Designs [C.E.D.], Cambridge, England), digitized (model 1401 AD/DA system, C.E.D.), analyzed (Spike 2 acquisition and analysis module, C.E.D.), and stored on magnetic media (personal computer). The following action potential parameters were analyzed: resting membrane potential, amplitude of phase 0, and action potential duration at 90% repolarization (APD_{90}). The maximal rate of rise of the action potential upstroke ($\dot{V}_{max}$) was measured with a differentiator adjusted for linearity within the range of 50 to 500 V/s.

Restitution of action potential characteristics was determined using single test pulses (S_2) delivered after every tenth basic beat (S_1). The S_1–S_2 coupling interval was increased progressively from the end of the refractory period until the next basic beat. Statistical analysis was performed using analysis of variance (ANOVA) coupled with the Bonferoni procedure. *d*-Sotalol (Bristol Myers) was dissolved in distilled water and used at a final concentration of 100 μM.

Results

Heterogeneity of transmembrane activity across the ventricular wall has been previously delineated in tissues isolated from the canine ventricle. Epicardial,

endocardial, and M cells differ principally with respect to repolarization characteristics. Epicardial and M cells commonly display a prominent early repolarization phase (phase 1) that is largely lacking in endocardium. Moreover, M cells differ from epicardial and endocardial cells with respect to phase 3 repolarization, displaying a greater prolongation of the action potential with slowing of the stimulation rate. These features of the three cell types are illustrated in the left panel of Figure 1A.

Effects of *d*-Sotalol on Rate Dependence of Action Potential Parameters

A representative example of the effects of *d*-sotalol on the rate-dependence of action potential morphology is shown in Figure 1. Each panel of Figure 1A shows superimposed traces recorded simultaneously from endocardial, epicardial, and midmyocardial regions of the canine left ventricle during field stimulation of the preparation at basic cycle lengths of 500, 1000, 2000,

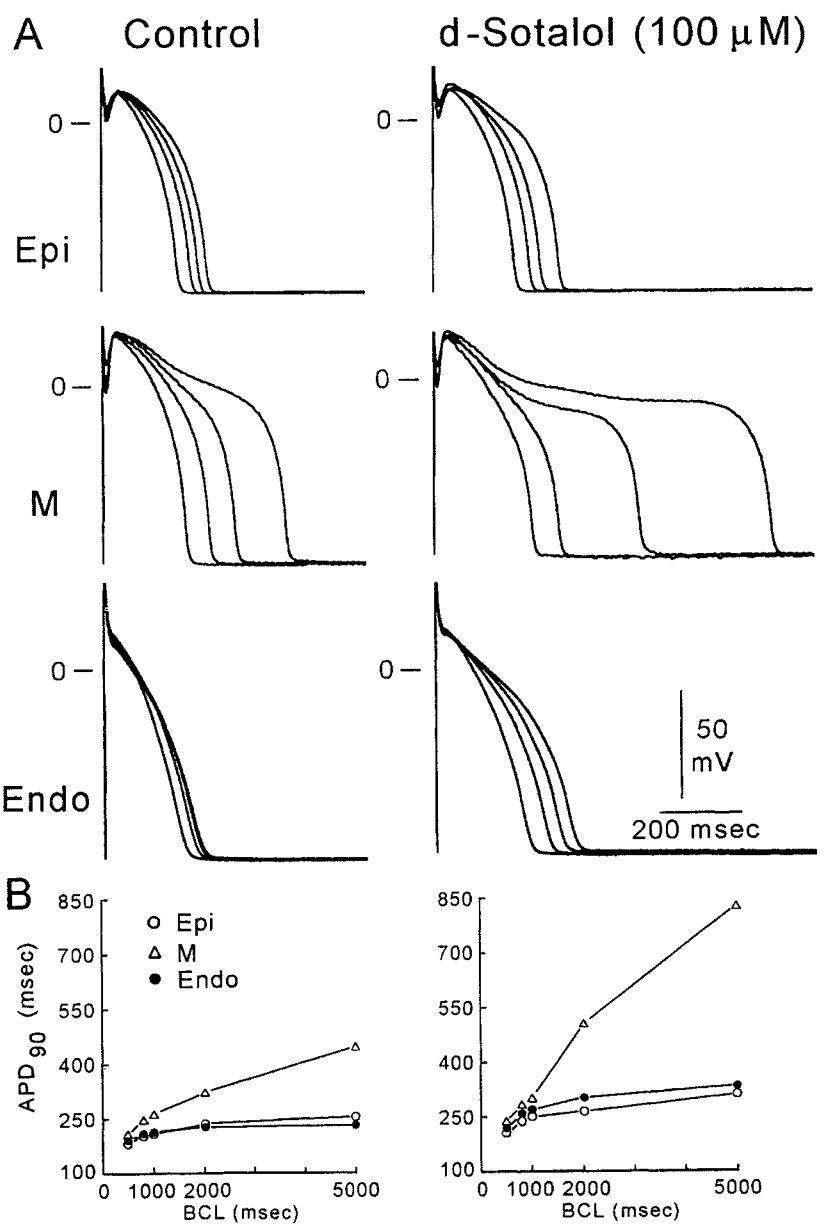

Fig. 1. Rate-dependent effects of *d*-sotalol in epicardial (Epi), M cell, and endocardial (Endo) preparations of the canine left ventricle. (A) Transmenbrane activity recorded simultaneously from Epi, M, and Endo before (control, left) and 30 minutes after exposure to 100 μM *d*-sotalol (right). The M cell was recorded from a transmural strip obtained by dermatome shaving made perpendicular to the epicardial surface 3 mm from the epicardial border. Recordings were obtained at basic cycle lengths of 500 ms, 1, 2, and 5 s (superimposed traces in each panel) under steady-state conditions. (B) Graphs displaying action potential duration (APD)-rate relations at each site before (left) and after *d*-sotalol (right). $[K^+]o = 4$ mM.

and 5000 ms under steady-state conditions. The recordings were obtained from a left ventricular transmural strip obtained by dermatome shaving made perpendicular to the epicardial surface, a dermatome shaving made parallel to the epicardial surface, and a dermatome shaving of the endocardial surface of the free wall. Under control conditions (left panel), the M cell display a longer action potential and a more accentuated rate-dependence of APD than epicardial and endocardial cells. *d*-Sotalol (right panel, 100 μM, 60 minutes of exposure) prolongs the action potential in the 3 cell types but more in the M cell than in the epicardial or endocardial cell, especially at the slower rates of stimulation. At a BCL of 5000 ms, APD_{90} increases 55 ms in epicardial cell (from 257 to 312 ms), 101 ms in endocardial (from 234 to 335 ms), but 378 ms in the M cell (from 450 to 828 ms). APDrate relations recorded in the same experiment are graphically illustrated in Figure 1B. Under control conditions (left panel) the M cell displays a steeper APD-rate relation than those of epicardium or endocardium. *d*-Sotalol (right panel) induces a steepening of APD-rate relations, especially of the M cell.

Composite data of the effects of *d*-sotalol on APD-rate relations recorded from 34 preparations isolated from 13 canine hearts are graphically illustrated in Figure 2. Following exposure to *d*-sotalol, a significant increase is observed in the APD of M cells at every cycle length ($P < 0.01$ *d*-sotalol vs control); at a BCL of 2000 ms APD_{90} increases from 199 ± 20 ms to 247.5 ± 28 ms in epicardial, from 212 ± 26 to 274 ± 27 ms in endocardial, and from 309 ± 65 to 533 ± 207 ms in M cells). *d*-Sotalol produces a marked steepening of APD-rate relations of M cells, resulting in an increase in the transmural dispersion of repolarization.

Table 1 summarizes the effects of *d*-sotalol on the action potential characteristics of the 3 cell types. *d*-Sotalol induces significant changes in APD_{90}, whereas the resting membrane potential, amplitude of phase 0, and maximal rate of rise ($\dot{V}_{max}$) remained relatively unchanged after drug administration.

Effects of *d*-Sotalol on Restitution of Action Potential Parameters

The data presented show that *d*-sotalol prolongs the action potential of M cells to a greater extent than that of either epicardial or endocardial cells under steady-state conditions. Because the determinants of APD may be different under nonsteady-state conditions, we evaluated the effects of *d*-sotalol on the characteristics of restitution of action potential in the different cell types. A representative example is illustrated in Figure 3. The M cell was recorded from a transmural dermatome shaving made perpendicular to the epicardial surface. Panel A displays superimposed traces of the basic beats (BCL = 2000 ms) followed by successive premature beats introduced at progressively longer S1–S2 intervals, once after every ten basic beats. Panel B plots APD_{90} of premature beats as a function of the diastolic interval for the same experiment. Under control conditions the restitution curve of M is displaced upward relative to that of epicardium and endocardium. *d*-Sotalol induces an upward shift of the 3 curves, more accentuated in the M cell. This and other similar experiments suggest that *d*-sotalol acts to prolong preferen-

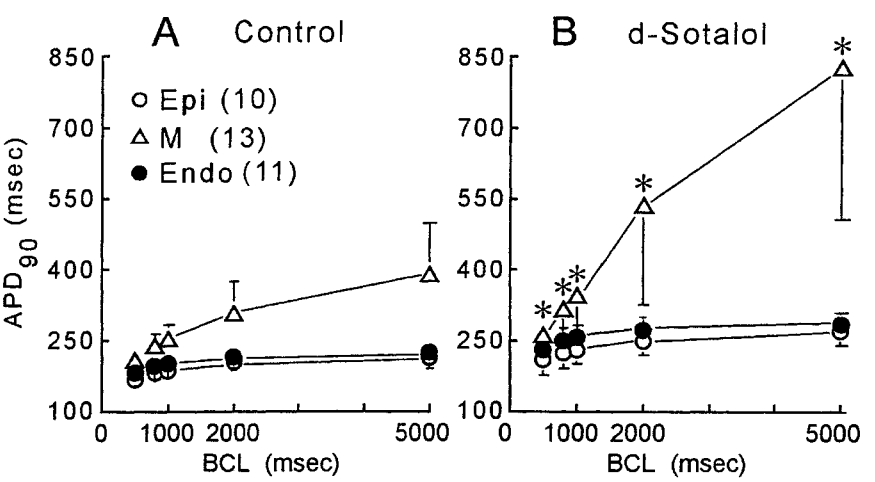

Fig. 2. Composite data of the rate-dependence effects of *d*-sotalol on action potential duration measured at 90% repolarization (APD_{90}) on epicardial (Epi), M cell, and endocardial (Endo) preparations isolated from the left ventricle of 13 canine hearts. The graphs plot APD-rate relations for Epi (open circles), Endo (closed circles), and M (open triangles) before (A) and after exposure to 100 μM *d*-sotalol (B). Each point represents mean ± SD. n = 10 for Epi, 11 for Endo, and 13 for M. *$P < .01$ *d*-sotalol vs control (ANOVA coupled with Bonferoni procedure). $[K^+]o = 4$ mM.

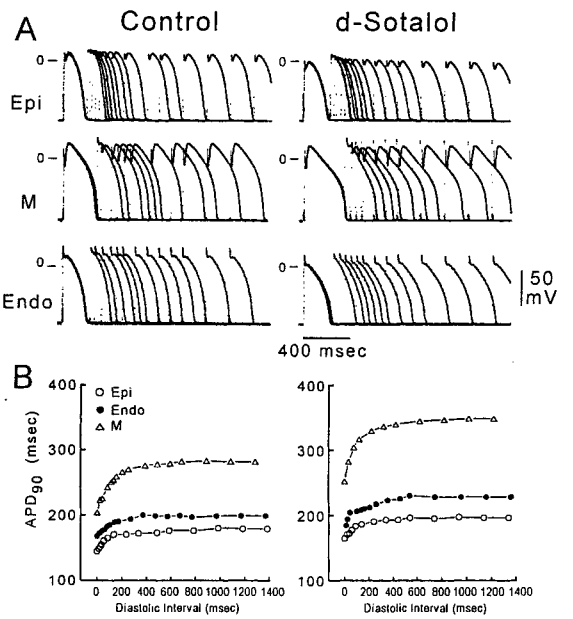

Fig. 3. Effects of *d*-sotalol on restitution of action potential in epicardial (Epi), M cell, and endocardial (Endo) preparations. (A) Transmenbrane activity recorded from Epi, M, and Endo before (control, left) and after exposure to 100 μM *d*-sotalol (right). The M cell was recorded from a transmural dermatome shaving at 2 mm from the epicardial border. In each panel the first action potential represents the basic beat elicited at a basic cycle length of 2,000 ms. Subsequent action potentials are premature beats elicited at different S1–S2 intervals. (B) Plots of action potential measured at 90% repolarization (APD_{90}) of premature beats as a function of the diastolic interval (interval between the end of the basic action potential and the upstroke of the premature response) at each site, before (left) and after exposure to 100 mM *d*-sotalol (right). $[K^+]o = 4$ mM.

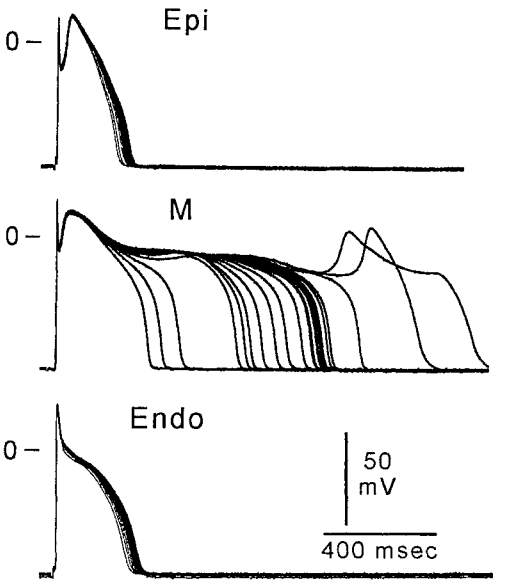

Fig. 4. *d*-Sotalol-induced early afterdepolarizations (EADs) and triggered activity in M cells, but not epicardial (Epi) or endocardial (Endo) preparations isolated from the canine left ventricle. Transmenbrane activities recorded from each site after 30 minutes of exposure to 100 μM *d*-sotalol following an abrupt change of rate from a basic cycle length of 800 ms (first action potential in each panel) to a basic cycle length of 8000 ms (subsequent action potentials). EAD-induced triggered responses are apparent only in the M cell. $[K^+]o = 4$ mM.

tially the M cells under steady-state as well as non-steady-state experimental conditions.

d-Sotalol Induces Early Afterdepolarizations and Triggered Activity in M Cells

In 7 of 13 M cell preparations (54%) EADs were observed 20–40 minutes following the introduction of 100 μM *d*-sotalol. Figure 4 shows superimposed traces recorded simultaneously from an epicardial, M cell, and endocardial preparation 30 minutes after exposure to 100 μM *d*-sotalol. The M cell was recorded from a parallel dermatome shaving at 2 mm from the epicardial surface. Following an abrupt slowing of the stimulation rate from a BCL of 800 ms (first beat in each panel) to a BCL of 8000 ms (subsequent beats), APD markedly increases in M but only slightly in epicardium and endocardium. The dramatic APD prolongation in the M cell is attended by the development of an EAD induced triggered response.

The rate-dependent changes of *d*-sotalol-induced triggered responses in M cells are further illustrated in Figure 5. A slowing of the stimulation rate from a BCL of 1200 ms to a BCL of 1400 ms results in the development of EAD-induced triggered response in every other stimulated beat (APD and EAD alternans) of the M cell preparation: beats following the longer pause (beat 1, 3, and 5) display EAD but not those following the shorter interval (beats 2, 4, and 6); further deceleration to a BCL of 1500 ms gives rise to triggered responses in every stimulated beat. Additional slowing to a BCL of 2200 ms leads to longer APDs and the reappearance of pause-dependent APD and EAD alternans.

Although marked action potential prolongation, EAD, and triggered activity were generally observed at slow rates of stimulation (BCL > 1000 ms) under steady-state conditions, a sudden acceleration of the rate could also induce a paradoxical transient prolongation of the action potential as illustrated in the example of Figure 6. Panel A plots the time course of APD changes following an abrupt acceleration of the

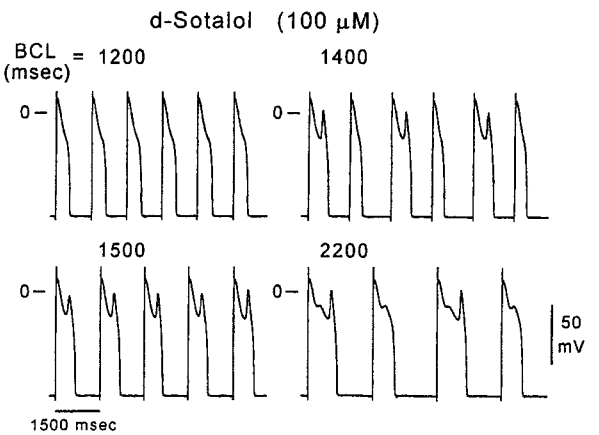

Fig. 5. Rate-dependence of *d*-sotalol-induced early afterdepolarizations (EAD) and triggered activity in M cells. Transmembrane activity recorded from an M cell preparation after 40 minutes of exposure to 100 μM *d*-sotalol at basic cycle lengths (BCL) of 1200, 1400, 1500, and 2200 ms under steady-state conditions. The M cell was recorded from a parallel dermatome shaving at 2 mm from the epicardial surface. At a BCL of 1400 ms (upper right), EAD-induced triggered responses in alternate beats; at a BCL of 1500 ms (lower left), EAD-induced triggered responses in every beat; at a BCL of 2200 ms (lower right), EAD alternating with EAD-induced triggered responses. $[K^+]o = 4$ mM.

rate recorded simultaneously from an epicardial and an M cell. The M cell was recorded from a transmural slice obtained by a dermatome shaving. Following acceleration of the rate from a BCL of 8000 ms to a BCL of 800 ms, an abrupt prolongation of APD_{90} is observed in the initial beats (407 ms, last beat at BCL = 8000 ms, to 574 ms, second beat at BCL of 800 ms), followed by a progressive decrease in APD, which reaches a steady-state only after 55 beats paced at a BCL of 800 ms; in contrast the epicardial cell only displays a progressive abbreviation of APD, which reaches a steady-state within 12 beats paced at a shorter BCL. The transient increase in APD following acceleration leads to a marked increase in the transmural dispersion of repolarization and the development of EAD activity (beats 3 to 5) in the M cell as illustrated in Figure 7B. *d*-Sotalol-induced APD prolongation and/or EAD following acceleration was observed in 4 of 7 M cell preparations where this effect was investigated.

Discussion

Our results demonstrate a preferential effect of the class III antiarrhythmic agent *d*-sotalol to prolong the action potential of M cells with respect to that of epicardial or endocardial cells. This effect was observed under steady-state and nonsteady-state (restitution) conditions and was more evident at the slower rates of stimulation. Early afterdepolarizations were observed in M cells but not epicardial or endocardial preparations following exposure to *d*-sotalol and a slowing of

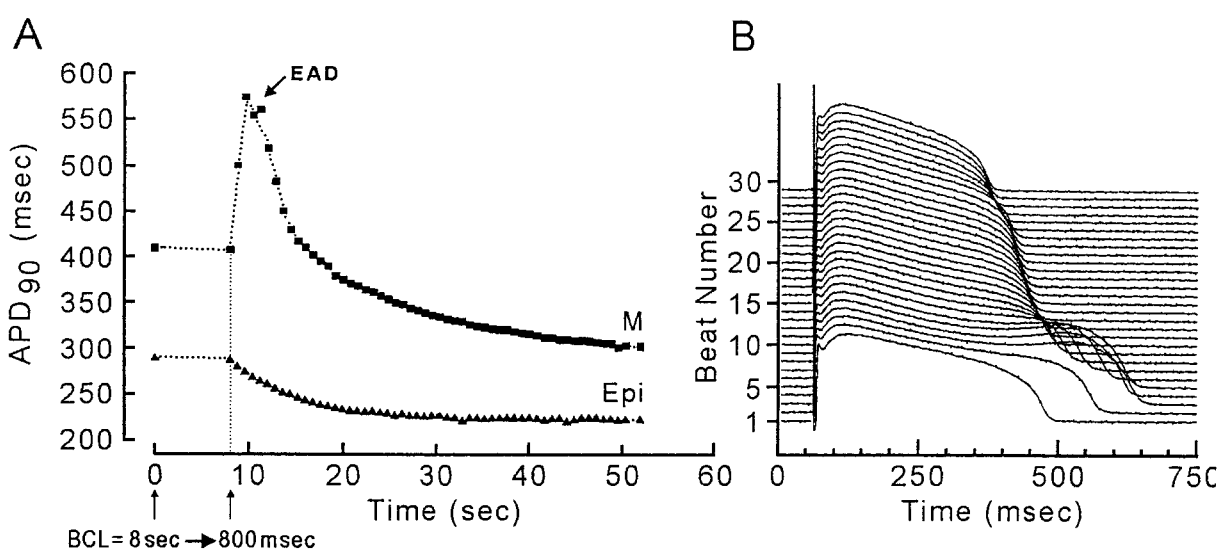

Fig. 6. *d*-Sotalol-induced action potential duration (APD) prolongation and early afterdepolarization (EAD) in M but not epicardial (Epi) tissues following acceleration. (A) Graph displaying time course of APD changes in M cell (closed circles) and Epi preparations following an abrupt acceleration from a BCL of 8000 ms (beats 1 and 2) to a BCL of 800 ms (subsequent beats) 30 minutes after exposure to 100 μM sotalol. (B) Transmembrane activity recorded from the M cell preparation. Beat 1(lower action potential) at a BCL of 8000 ms, following beats, BCL of 800 ms. APD prolongation and EAD are apparent only in M cell. $[K^+]o = 4$ mM.

the stimulation rate. Action potential prolongation and EADs were also observed in M cells in the initial beats following an abrupt increase in rate.

The main characteristic of the M cell is its ability to prolong disproportionately the action potential with respect to the other cell types (28). Action potentials with relatively long APDs have been first observed in the deep layers of papillary muscles of the canine ventricle (29) and in myocytes isolated from the rat ventricle (30). In the canine ventricle, M cells have been described and characterized in the deep subepicardial and midmyocardial layers of the free wall (23,28), deep subendocardial layers of the septum and papillary muscles (24), ventricular myocytes (31,32), and recently in arterially perfused wedge preparations (33,34), as well as in the canine heart *in vivo* (35–38). Others studies have presented evidence for the presence of M cells in the human (39) and guinea pig hearts (40,41).

d-Sotalol-induced Action Potential Duration Prolongation and Dispersion of Repolarization

Our data show that *d*-sotalol prolongs the action potential of M cells disproportionately to that of epicardial or endocardial cells (Figs. 1–3, Table 1). In addition, *d*-sotalol manifests its greatest effect at the slower rates and exerts much less effect at the faster rates. This effect, called reverse use-dependence (42), is common to most drugs with class III actions and is especially noticeable in M cells and Purkinje fibers due to the preferential effect of these agents on those tissues (20). The more pronounced effect of *d*-sotalol to prolong the M cell action potential with respect to the other cell types leads to a marked increase in the transmural dispersion of repolarization, especially at the slower rates of stimulation, setting the stage for possible reentrant arrhythmias and torsade de pointes (43). Our studies indicate no $\dot{V}_{max}$ depression (see Table 1), even at the faster rates, (BCL = 500 ms, data not shown). Although these results are similar to those observed in Purkinje fibers at the same concentration (100 μM) (14), Carmeliet (44) has reported a depression of $\dot{V}_{max}$ and shortening of the action potential at higher doses.

d-Sotalol Induced Afterdepolarizations and Triggered Activity

The effect of *d*-sotalol to produce EADs in M cells (Figs. 4–6) is similar to that previously observed in Purkinje fibers exposed to the same drug concentration (14). Similar results have been obtained with a variety of drugs with class III action. M cells, but not epicardial or endocardial cells, of the canine ventricle have been shown to develop EADs and EAD-induced triggered response following the exposure to several potassium channel blocker including quinidine, 4-aminopyridina, clofilium, cesium, amiloride, *dl*-sotalol, and calcium agonists (Bay K 8644), as well as agents that slow inactivation of I_{Na} (ATX II and Anthopleurin-A) (20,25,26). Similarly M cells but not epicardial or endocardial cells, of the guinea pig ventricle have been shown to exhibit EADs and triggered activity when exposed to *dl*-sotalol (40), and isolated guinea pig mycocytes displayed EADs following H1-receptor antagonists astemizole and terfenadine (45). The paradoxical *d*-sotalol-induced action potential prolongation and EAD activity following acceleration (Fig. 6) is similar to the results obtained with the I_{Kr} blocker E-4031 (46). The data correlate well with recent experimental and clinical studies show-

Table 1. Effects of *d*-Sotalol on Action Potential Parameters of Epicardial, M, and Endocardial Cells

BCL = 2000 ms	EPI (n = 10)	M (n = 13)	ENDO (n = 11)
RMP (−mv)			
Control	86 ± 4	89.5 ± 3	85 ± 4
d-Sotalol	85.5 ± 5	89 ± 4	86 ± 3
Phase 0 Amp (mv)			
Control	101 ± 6	108 ± 5	113 ± 8
d-Sotalol	100 ± 7	107 ± 6	110 ± 6
APD_{90} (ms)			
Control	199 ± 20	309 ± 65	212 ± 26
d-Sotalol	247.5 ± 28	533 ± 207*	274 ± 27
V_{max} (V/s)			
Control	178 ± 20	285 ± 47	202 ± 33
d-Sotalol	170 ± 25	269 ± 64	188 ± 27

BCL, basic cycle lengths; APD_{90}, action potential duration measured at 90% repolarization; EPI, epicardial; ENDO, endocardial; RMP, resting membrane potential; Phase 0 amp, phase 0 amplitude.

* $P < .01$ *d*-sotalol vs control (ANOVA coupled with Bonferoni procedure). All values are presented as mean ± SD. $[K^+]o = 4$ mM.

ing that precipitation of torsade de pointes is often preceded by an increase of rate and that acceleration-induced torsade episodes are often accompanied by the appearance of EAD-like deflections in monophasic action potential (47–50). Increase in sympathetic activity has also been shown to induce EAD-like activity in MAPs recorded from the left ventricular wall of patients with long QT syndrome (51,52).

Ionic Mechanisms

Liu and Antzelvitch (32) recently demonstrated the presence of two components of the delayed rectifier current in canine ventricular myocytes; I_{Kr}, a rapidly activated component blocked by E-4031, and I_{Ks}, a slowly activated component found to be significantly smaller in myocytes isolated from the M region. Distinct I_{Kr} and I_{Ks} components have been previously described in guinea pig ventricular myocytes (53) and recently in human myocytes (54). A weaker I_{Ks} may be in part responsible for the longer action potential of the M cell as well as to the greater response to class III agents including the development of EADs. *d*-Sotalol has been shown to exert its class III effects by blocking I_{Kr}, the rapid component of the delayed rectifier (53). I_{Kr} block by *d*-sotalol would result in a weaker outward repolarizing current and a prolonged action potential especially in M cells where I_{Ks} is relatively small (32). Recent preliminary studies have indicated that a larger late sodium current in M cells also sustains the long plateau of the M cell (55), therefore contributing to its long action potential at slow rates and response to drugs that prolong repolarization. Other preliminary studies have postulated an increase in the sodium–calcium exchanger, I_{Na-Ca}, as a basis for acceleration-induced EAD and APD prolongation following I_{Kr} block (56).

Physiologic and Clinical Implications

The presence of the M cells with ability to prolong their action potential dramatically and induce EADs in response to drugs or conditions that prolong repolarization may contribute importantly to the understanding of the mechanisms underlying the long QT syndrome, notched T waves, T wave alternans, pathophysiologic U waves, EAD-induced triggered activity, reentrant arrhythmias, and torsade de pointes (20).

Notched T waves and T wave alternans are frequent electrocardiographic manifestations of the long QT syndrome (57). A number of hypotheses have been formulated for the manifestations of T wave alternans (58). As delayed repolarization of M cells are thought to be responsible for the end of the T wave (34), our results (Fig. 6) suggest that alternating long and short M cell action potentials displaying no EAD activity may account for some T wave alternans phenomena observed in the clinics. In support of this hypothesis, using body surface mapping, Shimizu et al (59) recently reported that T wave alternans in a patient with long QT syndrome was related to heterogeneous repolarization mainly in the left frontal chest.

Torsade de pointes is a typical ventricular arrhythmia observed in both the congenital and acquired long QT syndrome. Recent *in vivo* studies involving intramural recordings in the dog have demonstrated the appearance of a marked increase in transmural dispersion of repolarization following exposure to prolonging repolarization agents (35,38) and have implicated subendocardial Purkinje fibers as the source of focal arrhythmia, and the M cells in the repetitive reentrant excitation circuits observed in torsade episodes following exposure to Anthopleurin-A (38). Intramural reentry has also been suggested as the mechanism of the maintenance of erythromycin-induced torsade de pointes in left ventricular wedge preparations (37).

A recent study on the effects of *d*-sotalol on mortality in patients with myocardial infarction was abruptly interrupted following a preliminary report indicating an increase in mortality in patients treated with *d*-sotalol as compared to the control group (19). The lack of significant beta-blocking properties of *d*-sotalol, as well as the proarrythmogenic effects owing to its reverse use-dependence effects on APD, preferential effects on M cells and Purkinje fibers, increased dispersion of repolarization, EAD-induced triggered activity in M cells and Purkinje fibers, and development of intramural reentry and torsade de pointes may contribute to the drug-induced proarrhythmogenic effects and increased mortality observed in the clinics.

While *d*-sotalol shares its propensity to proarrhythmia, including the development of torsade de pointes, with most class III agents, chronic amiodarone appears to be a rare exception (61). Its remarkable efficacy and very low incidence of proarrhythmia relative to that of other agents with class III actions may be due to the multiple effects of amiodarone (Na, K, Ca and β-blockade), which may account for a more homogeneous transmural action potential prolongation as compared to other class III agents (62) and to the absence of reverse use-dependence effects on APD (61). A recent report indicated that the sodium channel blocker mexitilene antagonizes the proarrhythmic effects of *d*-sotalol in an experimental model of torsade de pointes (63), suggesting that a combination of low doses of sodium blockade and I_{Kr} block may constitute a useful tool in the pharmacologic

treatment of ventricular arrhythmias and help avoid the proarrhythmic effects of class III agents.

Acknowledgments

We are grateful to Juan Escobar and Judy Hefferon for their skilled technical assistance, and to Drs. J. Di Diego and W. Shimizu for reading the manuscript.

References

1. Johnston GD, Finch MB, McNeil JA, Shanks RG. A comparison of the cardiovascular effects of (+)-sotalol and (+/–)-sotalol following intravenous administration in normal volunteers. Br J Clin Pharmacol 20:507, 1985
2. Lynch JJ, Wilber DJ, Montgomery DG, Hsieh TM, Patterson E, Lucchesi BR. Antiarrhythmic and antifibrillatory actions of the levo- and dextrorotary isomers of sotalol. J Cardiovasc Pharmacol 6:1132, 1984
3. Kwan YW, Solca AM, Gwilt M, Kane KA, Wadsworth RM. Comparative antifibrillatory effects of *d*- and *dl*-sotalol in normal and ischemic ventricular muscle of the cat. J Cardiovasc Pharmacol 5:233, 1990
4. Feld GK, Venkatesh N, Singh BN. Pharmacologic conversion and suppression of experimental canine atrial flutter: differing effects of *d*-sotalol, quinidine, and lidocaine and significance of changes in refractoriness and conduction. Circulation 74:197, 1986
5. Woosley RL, Barbey JT, Wang T, Funck-Brentano C. Concentration/response relations for the multiple antiarrhythmic actions of sotalol. Am J Cardiol 65:22A, 1990
6. Anastasiou-Nana MI, Gilbert EM, Miller RH, et al. Usefulness of *d*-sotalol, *l*-sotalol for suppression of chronic ventricular arrhythmias. Am J Cardiol 67:511, 1991
7. Hohnloser SH, Meinertz T, Stubbs P, et al. (For the *d*-Sotalol PVC Study Group) Efficacy and safety of *d*-sotalol, a pure class III antiarrhythmic compound, in patients with symptomatic complex ventricular ectopy. Circulation 92:1517, 1996
8. Gomoll AW, Lekich RF, Batek MJ, Comereski CR, Antonaccio MJ: Comparability of the electrophysiologic responses and plasma and myocardial tissue concentrations of sotalol and its *d* stereoisomer in the dog. J Cardiovasc Pharmacol 16:204, 1990
9. Brachmann J, Beyer T, Schmitt C, et al. Electrophysiologic and antiarrhythmic effects of *d*-sotalol. J Cardiovasc Pharmacol 20(II):91, 1992
10. Taggart P, Sutton PMI, Donaldson R: *d*-Sotalol: a new potent class III antiarrhythmic agent. Clin Sci 69:631, 1985
11. Shimizu W, Kurita T, Suyama K, Aihara N, Kamakura S, Shimomura K. Reverse use dependence of human ventricular repolarization by chronic oral sotalol in monophasic action potential recordings. Am J Cardiol 77:1004, 1996
12. Kato R, Ikeda N, Yabek M, Kannan R, Singh BN. Electrophysiologic effects of the levo- and dextrorotary isomers of sotalol in isolated cardiac muscle and their *in vivo* pharmacokinetics. J Am Coll Cardiol 7:116, 1986
13. Campbell TJ. Cellular electrophysiological effects of *d*- and *dl*-sotalol in guinea pig sinoatrial node, atrium, and ventricle and human atrium: differential tissue sensitivity. Br J Pharmacol 90:593, 1987
14. Hiromasa S, Coto H, Li ZY, Maldonado C, Kupersmith J. Dextrorotatory isomer of sotalol: electrophysiologic effects and interaction with verapamil. Am Heart J 116:1552, 1988
15. Dessertenne F. La tachycardie ventriculaire à deux foyers opposés variables. Arch Mal Coeur 59:263, 1966
16. Weissenburger J, Davy JM, Chezalviel F, et al. Arrhythmogenic activities of antiarrhythmic drugs in conscious hypokalemic dogs with atrioventricular block: comparison between quinidine, lidocaine, flecainide, propranolol, and sotalol. J Pharmacol Exp Ther 259:871, 1991
17. Singh SN, Lazin A, Cohen AJ, Johnson MC, Fletcher RD. Sotalol-induced torsade de pointes successfully treated with hemodialysis after failure of conventional therapy. Am Heart J 121:601, 1991
18. McNeil JA, Davies RO, Deitchman D. Clinical safety profile of sotalol in the treatment of arrhythmias. Am J Cardiol 72:44A, 1993
19. Waldo AL, Camm AJ, deRuyter H, et al. (and the Sword Investigators). Preliminary mortality results from the survival with oral *d*-sotalol (SWORD) trial. J Am Coll Cardiol 15A(Abstract), 1995
20. Antzelevitch C, Sicouri S. Clinical relevance of cardiac arrhythmias generated by afterdepolarizations: the role of M cells in the generation of U waves, triggered activity, and torsade de pointes. J Am Coll Cardiol 23:259, 1994
21. Antzelevitch C, Sicouri S, Lukas A, Nesterenko VV, Liu DW, Di Diego JM. Regional differences in the electrophysiology of ventricular cells: physiological and clinical implications. In Zipes DP, Jalife J (eds). Cardiac Electrophysiology: From Cell to Bedside. WB Saunders, Philadelphia. pp. 228–245, 1995
22. Antzelevitch C, Di Diego JM, Sicouri S, Lukas A. Selective pharmacological modification of repolarizing currents: antiarrhythmic and proarrhythmic actions of agents that influence repolarization in the heart. In Breithardt J (ed). Antiarrhythmic Drugs: Mechanisms of Antiarrhythmic and Proarrhythmic Actions. Springer-Verlag, Berlin. pp. 57–80, 1995
23. Sicouri S, Antzelevitch C. Electrophysiologic characteristics of M cells in the canine left ventricular free wall. J Cardiovasc Electrophysiol 6:591, 1995
24. Sicouri S, Fish J, Antzelevitch C. Distribution of M cells in the canine ventricle. J Cardiovasc Electrophysiol 5:824, 1994
25. Sicouri S, Antzelevitch C. Afterdepolarizations and triggered activity develop in a select population of cells (M cells) in canine ventricular myocardium: the effects of acetylstrophantidin and Bay K 8644. PACE 14:1714, 1991
26. Sicouri S, Antzelevitch C. Drug-induced afterdepolarizations and triggered activity occur in a discrete subpopulation of ventricular muscle cell (M cells) in the canine heart: quinidine and Digitalis. J Cardiovasc Electrophysiol 4:48, 1993

27. Moro S, Sicouri S, Nicola Siri L, Elizari MV: *d*-Sotalol produce un marcado aumento en la duracion de la repolarizacion y post despolarizaciones precoces en celulas M pero no en epicardicas ni endocardicas del ventriculo canino. Rev Arg Cardiol 63(I):227(Abstract), 1995
28. Sicouri S, Antzelevitch C: A subpopulation of cells with unique electrophysiological properties in the deep subepicardium of the canine ventricle: the M cell. Circ Res 68:1729, 1991
29. Solberg LE, Singer DH, Ten Eick RE, Duffin EG. Glass microelectrode studies on intramural papillary muscle cells. Circ Res 34:783, 1974
30. Watanabe T, Dellbridge LM, Bustamante JO, McDonald TF: Heterogeneity of the action potential in isolated rat ventricular myocytes and tissue. Circ Res 52:280, 1983
31. Liu DW, Gintant GA, Antzelevitch C: Ionic bases for electrophysiological distinctions among epicardial, midmyocardial, and endocardial myocytes from the free wall of the canine left ventricle. Circ Res 72:671, 1993
32. Liu DW, Antzelevitch C. Characteristics of the delayed rectifier current (I_{Kr} and I_{Ks}) in canine ventricular epicardial, midmyocardial, and endocardial myocytes: a weaker I_{Ks} contributes to the longer action potential of the M cell. Circ Res 76:351, 1995
33. Yan GX, Antzelevitch C. Delayed repolarization of M cells underlies the manifestation of U waves, notched T waves and long QT intervals in the electrocardiogram (ECG). Circulation 92:I-480(Abstract), 1995
34. Yan GX, Antzelevitch C. Cellular basis for the normal T wave and the electrocardiographic manifestations of the long QT syndrome. Circulation 92:1517, 1995
35. Weissenburger J, Nesterenko VV, Antzelevitch C. Intramural monophasic action potentials (MAP) display steeper APD-rate relations and higher sensitivity to class III agents than epicardial and endocardial MAPs: characteristics of the M cell *in vivo*. Circulation 92:I-300(Abstract), 1995
36. Weissenburger J, Nesterenko VV, Antzelevitch C. M cells contribute to transmural dispersion of repolarization and to the development of torsade de pointes in the canine heart *in vivo*. PACE 19:II-707(Abstract), 1996
37. Antzelevitch C, Sun ZQ, Zhang ZQ, Yan GX. Cellular and ionic mechanisms underlying erythromycin-induced long QT and torsade de pointes. J Am Coll Cardiol 28:1836, 1996
38. El-Sherif N, Caref EB, Yin H, Restivo M. The electrophysiological mechanism of ventricular arrhythmias in the long QT syndrome: tridimensional mapping of activation and recovery patterns. Circ Res 79:474, 1996
39. Drouin E, Charpentier F, Gauthier C, Laurent K, Le Marec H. Electrophysiological characteristics of cells spanning the left ventricular wall of human heart: evidence for the presence of M cells. J Am Coll Cardiol 26:185, 1995
40. Sicouri S, Quist M, Antzelevitch C. Evidence for the presence of M cells in the guinea pig ventricle. J Cardiovasc Electrophysiol 7:503, 1996
41. Main MC, Bryant SM, Hart G. Electrical and mechanical characteristics of guinea pig left ventricular midmyocardial myocytes compared with surface myocytes. J Physiol 483:9P, 1995
42. Hondeghem LM, Snyders DJ. Class III antiarrhythmic agents have a lot of potential but have a long way to go: reduced effectiveness and dangers of reverse use dependence. Circulation 81:686, 1990
43. Surawicz B: Electrophysiologic substrate of torsade de pointes: dispersion of repolarization or early afterdepolarizations? J Am Coll Cardiol 14:172, 1989
44. Carmeliet E. Electrophysiology and voltage clamp analysis of the effects of sotalol on isolated cardiac muscle and Purkinje fibers. J Pharmacol Exp Ther 232:817, 1985
45. Salata JJ, Jurkiewicz NK, Wallace AA, Stupienski RF, Guinosso PJ, Lynch JJ. Cardiac electrophysiological actions of the histamine H_1-receptor antagonists astemizole and terfenadine compared with chlorpheniramine and pyrilamine. Circ Res 76:110, 1995
46. Burashnikov A, Antzelevitch C. Acceleration-induced early afterdepolarizations and triggered activity. Circulation 92:I-434(Abstract) 1995
47. Jackman WM, Friday KJ, Anderson JL, Aliot EM, Clark MA, Lazzara R. The long QT syndromes: a critical review, new clinical observations, and a unifying hypothesis. Prog Cardiovasc Dis 2:115, 1988
48. Habbab MA, El-Sherif N. TU alternans, long QTU, and torsade de pointes: clinical and experimental observations. PACE 15:916, 1992
49. Locati EH, Maison-Blanche P, Dejode P, Cauchemez B, Coumel P. Spontaneous sequences of onset of torsade de pointes in patients with acquired prolonged repolarization: quantitative analysis of Holter recordings. J Am Coll Cardiol 25:1564, 1995
50. Vos MA, Verduyn SC, Gorgels APM, Lipcsei GC, Wellens HJ: Reproducible induction of early afterdepolarizations and torsade de pointes arrhythmias by *d*-sotalol and pacing in dogs with chronic atrioventricular block. Circulation 91:864, 1995
51. Shimizu W, Ohe T, Kurita T, et al. Early afterdepolarizations induced by isoproterenol in patients with congenital long QT syndrome. Circulation 84:1915, 1991
52. Shimizu W, Ohe T, Kurita T, Tokuda T, Shimomura K. Epinephrine-induced ventricular premature complexes due to early afterdepolarizations and effects of verapamil and propranolol in a patient with congenital long QT syndrome. J Cardiovasc Electrophysiol 5:438, 1994
53. Sanguinetti MC, Jurkiewicz NK. Two components of cardiac delayed rectifier K^+ current: differential sensitivity to block by class III antiarrhythmic agents. J Gen Physiol 96:195, 1990
54. Li GR, Feng J, Yue L, Carrier M, Nattel S: Evidence for two components of delayed recifier K^+ current in human ventricular myocytes. Circ Res 78:689, 1996
55. Eddlestone GT, Zygmunt AC, Antzelevitch C. Larger late sodium current contributes to the longer action potential of the M cell in canine ventricular myocardium. PACE 19:II-569(Abstract), 1996
56. Burashnikov A, Antzelevitch C. Mechanism of acceleration-induced early afterdepolarization activity and action potential prolongation in tissues isolated from the M region of the canine ventricular. PACE 19:II-645 (Abstract), 1996

57. Zareba W, Moss AJ, Le Cessie S, Hall WJ. T wave alternans in idiopathic long QT syndrome. J Am Coll Cardiol 23:1541, 1994
58. Surawicz B, Fisch C. Cardiac alternans: diverse mechanisms and clinical manifestations. J Am Coll Cardiol 20:483, 1992
59. Shimizu W, Kamakura S, Arakaki Y, Kamiya T, Shimomura K. T wave alternans in idiopathic long-QT syndrome: insight from body surface mapping. PACE 19: 1130, 1996
60. Hohnloser SH, Klingenheben T, Singh BN: Amiodarone-associated proarrhythmic effects: a review with special reference to torsade de pointes tachycardia. Ann Intern Med 121:529, 1994
61. Sicouri S, Moro S, Nicola Siri L, Elizari MV, Litovsky SH, Antzelevitch C. Chronic amiodarone delays ventricular repolarization and reduces transmural dispersion of repolarization in the canine heart. PACE 19:II-638(Abstract), 1996
62. Sager PT, Uppal P, Follmer C, Antimisiaris MG, Pruitt CM, Singh BN. Frequency-dependent electrophysiologic effects of amiodarone in humans. Circulation 88:1063, 1993
63. Chezalviel-Guilbert F, Davy JM, Poirier JM, Weissenburger J. Mexiletine antagonizes effects of sotalol on QT interval duration and its proarrhythmic effects in a canine model of torsade de pointes. J Am Coll Cardiol 26:787, 1995